Available online at sjuoz.uoz.edu.krd

Science Journal of University of Zakho
Vol. 12, No. 1, pp. 14 – 21 January-March, 2024

p-ISSN: 2410-7549
e-ISSN: 2414-6943

ELECTRICAL, OPTICAL, AND CHEMICAL PROPERTIES OF GRAPHENE THIN FILMS FABRICATED BY VACUUM FILTRATION TECHNIQUE

Shivan H. Haji, Faris A. Kochary, Sabah M. Ahmed
Department of Physics, College of Science, University of Duhok, Duhok, Kurdistan Region of Iraq
(shivanhasanhaji89@gmail.com , fkochary@uod.ac, sabma62@uod.ac)

Received: 4 Sep., 2023 / Accepted: 3 Oct., 2023 / Published: 15 Jan., 2024. https://doi.org/10.25271/sjuoz.2024.12.1.1198

ABSTRACT:

There has been considerable interest in graphene as a transparent electrode material because of its extraordinary features, such as high optical transmittance, high electrical conductivity, excellent thermal conductivity, exceptional mechanical strength, and remarkable electrochemical capacity. In addition, transparent conductors' graphene thin films have been considered a promising candidate to replace currently utilized indium tin oxide films, which are unlikely to meet future demands because of their rising cost. In this study, a vacuum filtration process along with isopropyl alcohol (IPA)-assisted with direct transfer (IDT) technique is used to prepare wide-area highly conductive graphene thin films on different substrates including (glass, and PET). The graphene thin films' optical, structural, and electrical properties are studied. The graphene sheets are deposited homogeneously on the substrate, and the distribution of small graphene sheets is observed in SEM images. XPS analysis revealed that the amount of oxygen in graphene decreases significantly with annealing at 500°C and treated with HNO3. Furthermore, the graphene transparent conductive films prepared by the adjusted vacuum filtration method show low sheet resistances of 12.2, 1.41, 1.18, and 0.8 kΩ/sq with transmittances of 81%, 70%, 64.3%, and 46.4% respectively after being annealing at 500°C and treated with HNO3.

KEYWORD: Graphene Thin Film, Vacuum Filtration, IPA-assisted Direct Transfer, Electrical Resistivity, Optical Transparency.

1. INTRODUCTION

One of the biggest challenges in the field of organic electronics is to develop reliable techniques for manufacturing highly conductive, flexible, and transparent electrodes (Southard et al., 2009). Indium tin oxide (ITO) is the most commonly employed transparent electrode due to its optical transparency, exceeding 80% in the visible light spectrum. It also possesses a low sheet resistance ranging from 10 to 30 Ω/sq and a favorable work function of around 4.8 eV (Wang et al., 2008)(Kim et al., 2007).

However, Indium Tin Oxide (ITO) has certain drawbacks, including sensitivity to basic and acidic conditions, elevated surface roughness, and rising costs caused by the lack of indium. Furthermore, ITO exhibits brittleness, leading to micro-cracks formation when subjected to bending stress and a dramatic reduction in conductivity. During the previous decade, extensive research was concentrated on developing modern kinds of flexible electrode materials to substitute the conventional ITO (Parvez et al., 2013). The search for new electrode materials has yielded several significant results, including the discovery of graphene, metal gratings, random networks of metallic nanowires, and carbon nanotubes (CNTs) (Kumar & Zhou, 2010)(De et al., 2009).

Graphene is a widely recognized type of two-dimensional carbon monolayer that consists of all sp2-hybridized carbons (W. Zhang et al., 2020). It has fascinating properties, such as being lightweight, having high thermal and electrical conductivity, exhibiting a highly tunable surface area close to 2675 m^2g^{-1}, having strong mechanical strength close to 1TPa, and showing chemical stability(J. Xia et al., 2009)(Lee et al., 2008). Its remarkable and outstanding properties make it an excellent, promising candidate for electronics, performance structural nanocomposites, and advanced environmental protection and energy devices, which include both storage and energy generation(J. Liang et al., 2009) (Pumera, 2010). The outstanding physical and chemical properties of graphene material also make it highly attractive for sustainable energy generation and electrochemical energy storage(Olabi et al., 2021). It is used in Li-ion batteries, super capacitors, fuel cells, photovoltaic, solar cells, and triboelectric nanogenerators (TENG) (Simon & Gogotsi, 2008).

Lately, there has been extensive exploration of numerous strategies based on bottom-up or top-down synthesis methods to obtain graphene sheets (Gutiérrez-Cruz et al., 2022). Bottom-up approaches are utilized to efficiently synthesize high-quality graphene that utilizes surface-assisted coupling of precisely selected molecular precursors on high-quality metal catalyst substrates by using chemical vapor deposition and epitaxial growth techniques on the wafer scale.(Bae et al., 2010)(Z. Xia et al., 2016).

The creation of graphene on a large scale through the methods mentioned above is impeded by several challenges, including difficulties in achieving high-temperature control over the cooling rate, the requirement for high-quality substrate materials, and managing the pressure (Vasanthi et al., 2020). The top-down approaches have enabled direct natural or synthetic graphite exfoliation into single or few-layer graphene in the liquid phase. A variety of effective top-down methods, including high-shear mixing, liquid sonication, electrochemical exfoliation, and reduction of graphite oxide, were employed for the mass production of high-quality graphene sheets at the gram and even at kilogram scales(Yang et al., 2016)(Z. Y. Xia et al., 2014).

* Corresponding author

Graphene is widely considered a highly promising option for flexible electronics because it has a remarkably tunable bandgap and a large surface area with unique 2D structures due to its atomic thickness(Nair et al., 2008)(Bae et al., 2010). The arrangement of graphene sheets mainly creates extensive thin films, which are ideal for integrating and designing flexible devices. A variety of techniques have been utilized in the past to create graphene thin films, for example, Langmuir–Blodgett (LB) assembly, layer-by-layer (LbL) assembly, dip coating, drop casting, spin coating, rapid freezing via spraying, dry/ solution-based transfer techniques, as well as inkjet, screen, and gravure printing(Han et al., 2013)(Eda, Fanchini, et al., 2008b).

However, leaving residual dispersion agents on the surface of graphene thin films made by the LbL and LB assemblies technique is a common problem that causes a significant increase in contact resistances and affects the electrical properties of graphene thin film. The graphene thin films made by drop casting, spin coating, and dip coating techniques also suffer from uncontrollable thickness, low efficiency, and inhomogeneity. Additionally, gravure printing and Ink-jet screen methods necessitate the use of additives like polymers to regulate the level of viscosity, which can have negative influences on the optical and electrical properties of graphene thin films.(Baptista-Pires et al., 2016).

These methods also necessitate high-temperature to anneal the films and remove the additives, which is not appropriate with flexible substrates such as paper, plastic, PET, and textiles (Baptista-Pires et al., 2016). Therefore, it is essential to create methods for depositing graphene films on a particular substrate without the use of additives. The technique of vacuum filtration is widely used for making highly flexible and durable wearable electronics, and it is also extensively used for the successful deposition of high-quality films composed of versatile and exceptional materials such as carbon nanotubes and graphene(Su et al., 2011). It is a considerably simple technique that has the capability of controlling the thickness and number of layers in a thin film, as well as achieving a significantly homogeneous surface of the thin film(Eda, Fanchini, et al., 2008a).

A novel method for transferring graphene film filtration membrane using an IPA-assisted direct transfer process was developed. This process allows for easy transfer of Graphene films to various substrates, including paper, fibers, polymeric sheets, Si, PET, and glass substrates for further use. The homogeneous transparent conductive graphene films have been fabricated through vacuum filtration technique and subsequent transfer to the desired substrates with low sheet resistances of 12.2, 1.41, 1.18, and 0.8 kΩ/sq and transmittances of 81%, 70 %, 64.3%, and 46.4% respectively, after being annealed at 500°C and treated with HNO_3.

2.EXPERIMENTAL SECTION

2-1 Materials

Pure graphene (ca. 98%) powders were bought from Nanjing XFNANO Materials Tech Co., Ltd. Additionally, N, N-Dimethylformamide DMF (Sigma Aldrich, 99%) was utilized as a solvent. Moreover, isopropyl alcohol IPA (99.8%, Sigma-Aldrich) was used to separate the graphene thin film from the membrane. Furthermore, acetone ACE (99.9%, Sigma-Aldrich) was employed to clean tools. Additionally, nitric acid HNO3 (Sigma Aldrich, 99.5%) was used to treat graphene thin films. Lastly, polytetrafluoroethylene PTFE (47 mm, 25nm) was bought from Beijing Shenghe Tech Co., Ltd.

2-2 Graphene Thin Film Formation

Initially, 2.5 mg of graphene powder was added to 100 mL of N, N-Dimethylformamide (DMF) solution. An ultrasonic path was used to mix the solution with graphene powders at room temperature for 4 h. Graphene aggregation was removed by centrifuging the suspended solution at 8000 rpm for 10 min. The well-dispersed graphene suspension had a 0.025 mg/mL concentration, as illustrated in Figure (1). Next, graphene solutions of numerous volumes (4, 8, 16, and 24 mL of 0.025 mg/mL) were first filtered through a polytetrafluoroethylene (Teflon PTFE) 25nm porous membrane with a (diameter of 47mm) to create filtered graphene films. The filtered graphene film was dipped several times in deionized water to remove any residual DMF and graphene fragments. The filtered graphene film had strong interlayered interactions of graphene. It retained the original circular shape, which was the same size as the filtration membrane (d = 47 mm). The filtered graphene film was invulnerable to surface tension and could be transferred to any target substrate for further applications and device construction.

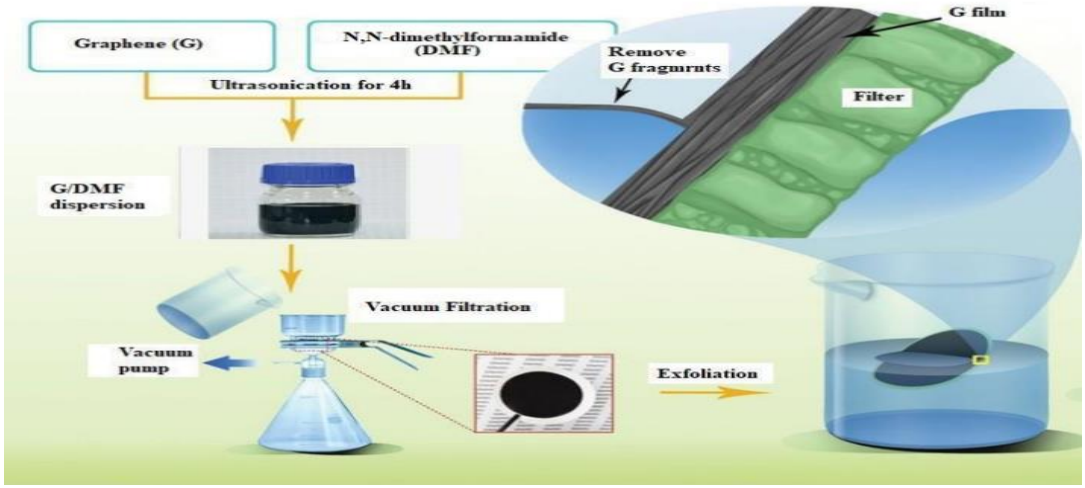

Figure 1: Demonstration steps of preparing graphene thin film .

2-3 Transferring process of graphene thin film to substrate

Filtered graphene film on hydrophilic polytetrafluoroethylene (PTFE) membrane has been transferred on different cleaned substrates (referred to as (M/G/IPA/Sub"). The steps of

transferring the filtered graphene film are illustrated in Fig (2). Fig (3(a, b)) reveals the filtered graphene films on the PTFE membrane and filter paper substrates respectively. Fig (3(c, d)) shows the transferred filtered graphene films onto PTE and glass substrates respectively.

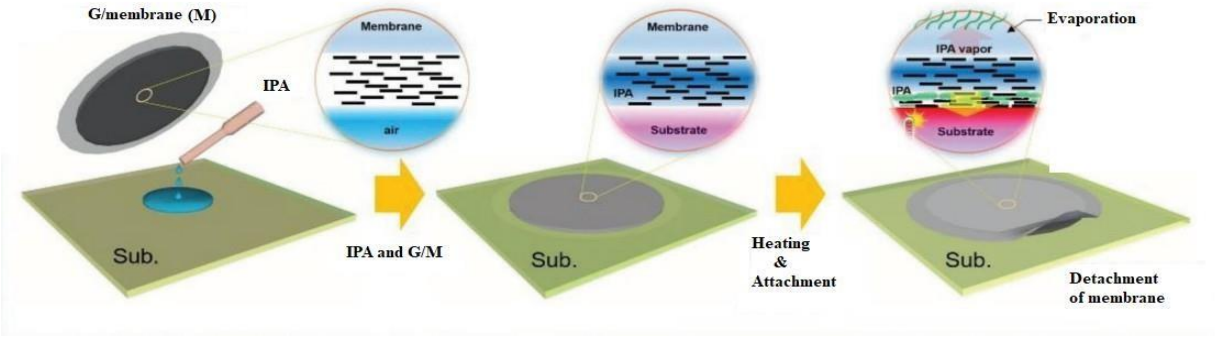

Figure 2: Represents the steps of transferring the graphene film onto a substrate.

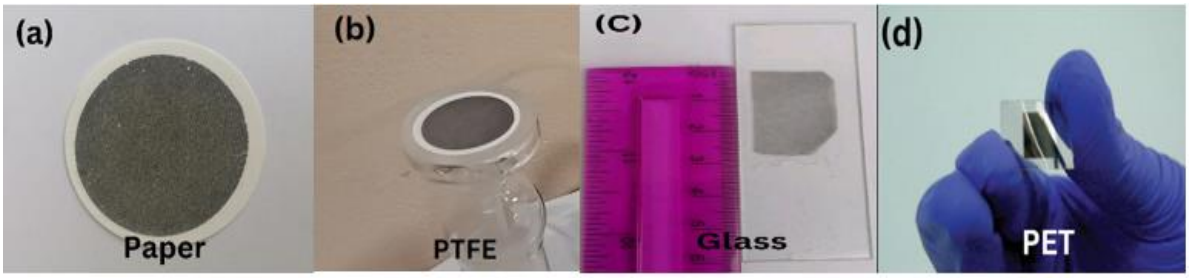

Figure 3: Filtered graphene films on a) PTFE membrane, b) filter paper. Transferred graphene film on a variety of substrates such as, such as c) glass, d) PET.

2-4 Annealed process and nitric acid treatment

The grown graphene thin films versus transmittance curves were analyzed under different processing conditions. This included natural drying, vacuum drying at 200°C, and annealing at 500°C following vacuum drying at 200°C. Furthermore, the effects of treating the annealed films at 500°C with HNO_3 were examined.

2-5 Characterization

X-ray diffraction (XRD) measurements were carried out using a PAN analytical X' Pert PRO (Cu Kα = 1.5406 Å) to identify the crystallographic structure. The structure and morphology of the graphene thin films were also examined with a scanning electron microscope (SEM) (Quanta 450). Additionally, X-ray photoelectron spectroscopy (XPS, ESCALAB 250) was used to analyze the surface chemical components of as prepared graphene thin films and treated with HNO_3 graphene thin films. The chemical composition of the graphene powder and as prepared graphene thin films was measured by EDX (Energy Dispersive X-ray Spectroscope) performed in SEM. Furthermore, the sheet resistances and transmittance of graphene thin film were measured by Keithly2450 four-point probe and 6850 UV spectrophotometer, respectively.

3-RESULTS AND DISCUSSION

3-1 Structural Properties and Morphology

The XRD pattern of graphene thin film with 70 % transparency is shown in Figure (4). The X-ray diffraction peak of thin graphene film is obtained at 26.3°, corresponding to the plane (002), which is typical of the hexagonal crystal structure(Chen et al., 2011). The graphene thin film corresponding inter-planar distance (d) obtained from XRD information is 3.39 Å. Comparatively, the inter-planar distance of the graphene thin film is slightly larger than that of the standard graphite powder 3.35 Å, with a difference of 0.04 Å(Siberian et al., 2018). This difference in the inter-planar distance of the thin graphene film from that of graphite powder shows that the vacuum filtration method effectively prevents the re-aggregation of graphene into graphite during the preparation of the thin film from the exfoliated graphene dispersion. High intensity and sharp diffraction peaks show that the graphene crystalline thin films have high quality.

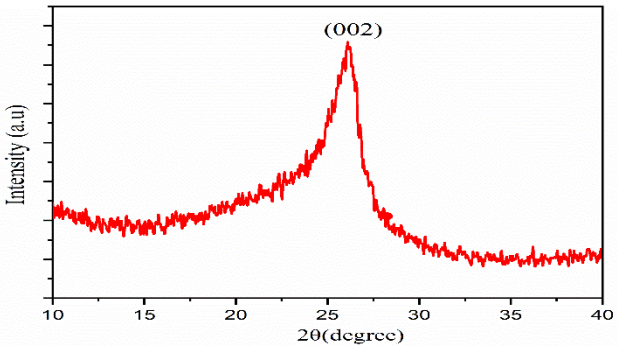

Figure 4: The XRD pattern of a graphene thin film

In Figure (5), Scanning electron microscope (SEM) was used to analyze the microstructure of the as-prepared graphene thin films. The typical SEM images of graphene thin films observed that the graphene nanosheets were stacked and overlapped to shape a conducting platform with the continuous graphene thin film for the movement of charge carriers. The scanning electron microscope (SEM) images depict the graphene thin film on a glass substrate at various locations, demonstrating that the graphene nanosheets uniformly homogenously coat the entire surface of the glass substrate. The continuous and uniform homogenously coating graphene thin film suits applications requiring effective conductivity, such as electronic devices or sensors(Wang et al., 2015).

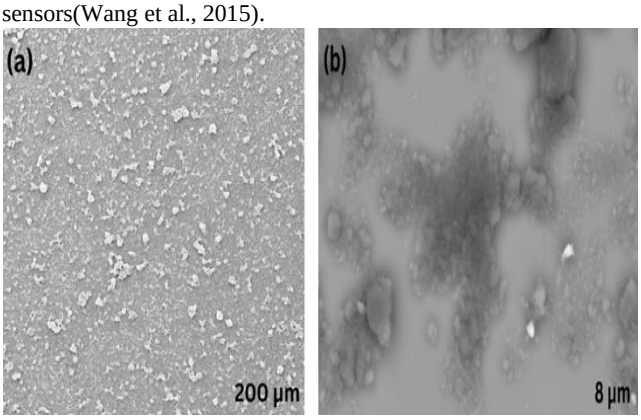

Figure 5: Images of the graphene thin film (a, b) Obtained by SEM.

From the SEM images, it is also observed that there are no cracks or crashes on the surface of the film. The absence of cracks demonstrates that the film sustains its structural integrity, making it acceptable for several applications when solidity is fundamental. Additionally, cracks can impair the mechanical durability of a substance and direct to failure under stress(Hwangbo et al., 2014). For that reason, the absence of cracks illustrates that the graphene thin film has good mechanical strength(Rafiee et al., 2010)(P. Zhang et al., 2014). Furthermore, graphene is famous for having excellent electrical conductivity, but cracks on the surface can damage the inflow of electrons, decreasing total conductivity. Hence, a crack-free graphene thin film possesses a more significant opportunity to conserve its electrical conductivity, which is beneficial for optoelectronic and electronic devices. Moreover, the absence of cracks reveals a smooth surface, which gives better adhesion, contact, and interconnect interaction with other materials or devices(Kholmanov et al., 2012)(X. Liang et al., 2011). Also, it can provide developed optical properties, for example, decreased scattering or improved light transmission. In total, noticing a crack-free graphene thin film shows the successful manufacturing of high-quality material, ensuring reliable and consistent performance, which is essential for research fields and industries depending on graphene for various applications(Cai et al., 2016).

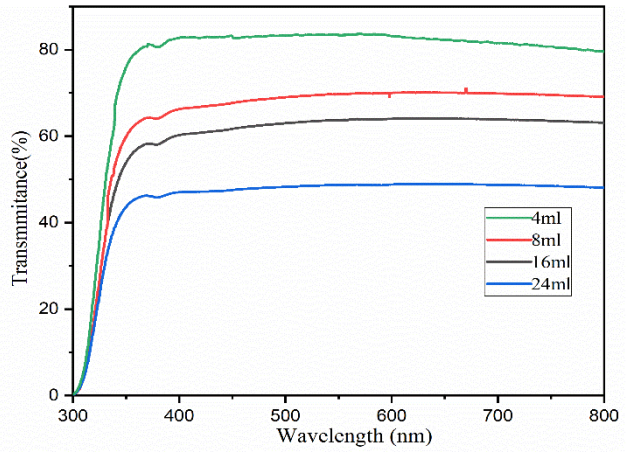

Figure 6: Transmittance spectra of graphene thin films obtained with 4mL,8 mL,16 mL, 24 mL graphene dispersion.

3-2 Optical Properties

UV spectrophotometer has been used to measure the optical properties of graphene thin films. Figure (6) illustrates the optical transmittance spectra (T) (300-1100 nm range) of graphene thin films deposited in glass substrates. Transmittance measurements were carried out on films fabricated from various volumes of graphene dispersions, particularly 4mL, 8mL, 16 mL, and 24 mL. With these volumes, transmittance values of 81%, 70%, 64.3%, and 46.4% were obtained at a wavelength of 550 nm, respectively. There was a decrease in the transmittance of the resulting films as the volume of the graphene dispersion increased. Thick films tend to absorb, reflect and scatter more light, which reduces the quantity of light that can flow through the graphene thin films(Jo et al., 2012).

3-3 Elementary Composition and Electrical properties

Figure (7a) reveals the EDX analysis of pure graphene powder used in this work. It has been shown that graphene is composed of 100% carbon and no oxygen. In addition, Figure (7b) illustrates EDX mapping images of the carbon, which indicates the absence of oxygen.

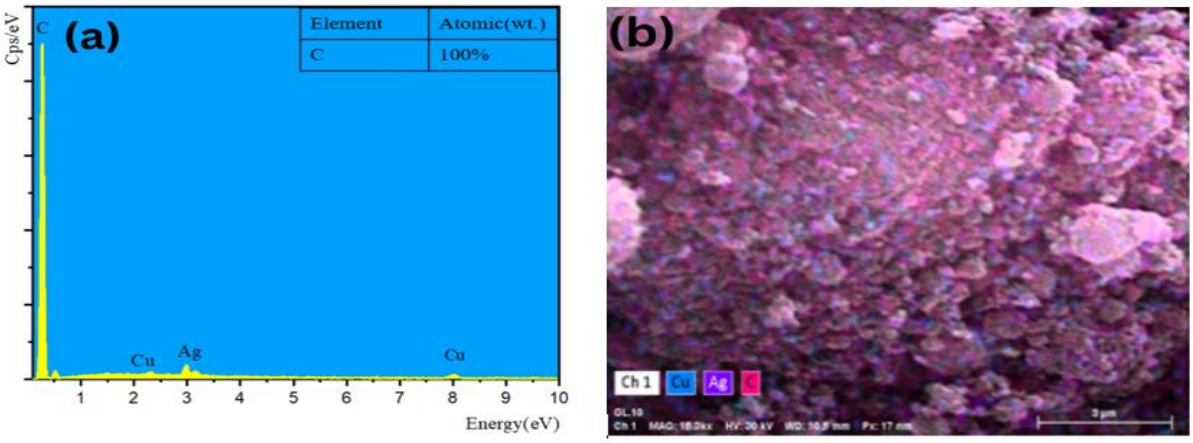

Figure 7: a) EDX of graphene powder. b) EDX mopping analysis of graphene.

EDX element composition. From the Figure, one can notice a peak of oxygen with a high percentage appearing. The contained oxygen comes from the alkaline chemicals used to prepare the thin film. However, some oxygen might have come from the atmosphere during graphene thin film preparation as it is chemically approved that the carbon and oxygen have an excellent electronic affinity(Ito et al., 2008)(Kadhim & Mohammed, 2022).

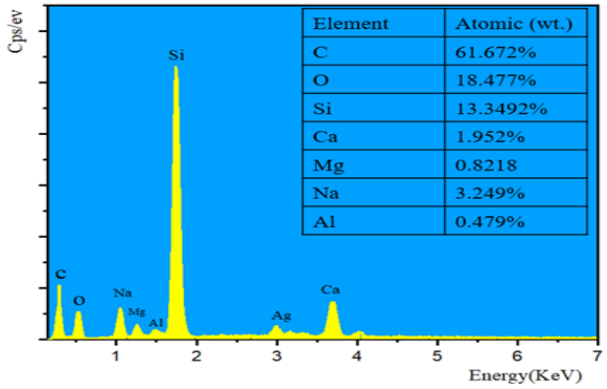

Figure 8: The EDX of as prepared graphene thin films.

Keithely 2450 four probes have been used to measure the electrical resistance of graphene thin films. Resistance measurements were carried out on as prepared graphene thin films fabricated from various volumes of graphene dispersions, particularly 4mL, 8mL, 16 mL, and 24 mL. With these volumes, resistance values of 1000 kΩ/sq, 200 kΩ/sq, 90.5 kΩ/sq, and 21.12 kΩ/sq were obtained, respectively, as demonstrated in Table (1). This high resistance may be due to the presence of residual N_N demathyleformide solvent(Shi et al., 2015). Another reason observed is coming from the results of the XPS technique, as shown in Figure (9a), which informs that a bond between the carbon and oxygen (C-O) appeared at 285.9 eV when fabricating the graphene thin film. The amount of O is high, about 23% (wt) weight percent, and C is about 77% (wt) weight percent as shown in Figure (10)(Li et al., 2016).

Table (1)

Volume of graphene dispersion	Transmittance of graphene thin films	Resistance of as prepared graphene thin films	Resistance of graphene thin films vacuum dried at 200°C	Resistance of graphene thin films annealed at500°C after dried at 200°C	Resistance of graphene thin films treated with HNO3 after annealed at 500°C
4mL	81%	1000 kΩ/sq	420 kΩ/sq	55 kΩ/sq	12.2 kΩ/sq
8mL	70%	200 kΩ/sq	80.1 kΩ/sq	10.3 kΩ/sq	1.41 kΩ/sq
16mL	64.3%	90.5 kΩ/sq	20.4 kΩ/sq	3.5 kΩ/sq	1.18 kΩ/sq
24mL	46.4%	21.12 kΩ/sq	14 kΩ/sq	1.6 kΩ/sq	0.8 kΩ/sq

The thin films, after being dried at 200°C under vacuum conditions, the residual of N_N demathyleformide solvent was eliminated, resulting in lower sheet resistance values of 420 kΩ/sq, 80.1 kΩ/sq,20.4 kΩ/sq, and 14 kΩ/sq, respectively as shown in Table (1)(Su et al., 2011). Then, the graphene thin films were annealed at a temperature of 500°C, and the resistance of the thin films significantly decreased to (55 kΩ/sq , 10.3 kΩ/sq, 3.5 kΩ/sq, 1.6 kΩ/sq) respectively, as shown in Table (1)(Xueshen et al., 2013). This significant decrease in sheet resistance may be due to a dramatic reduction in the C-O bond and other chemical defects(Eda, Lin, et al., 2008)

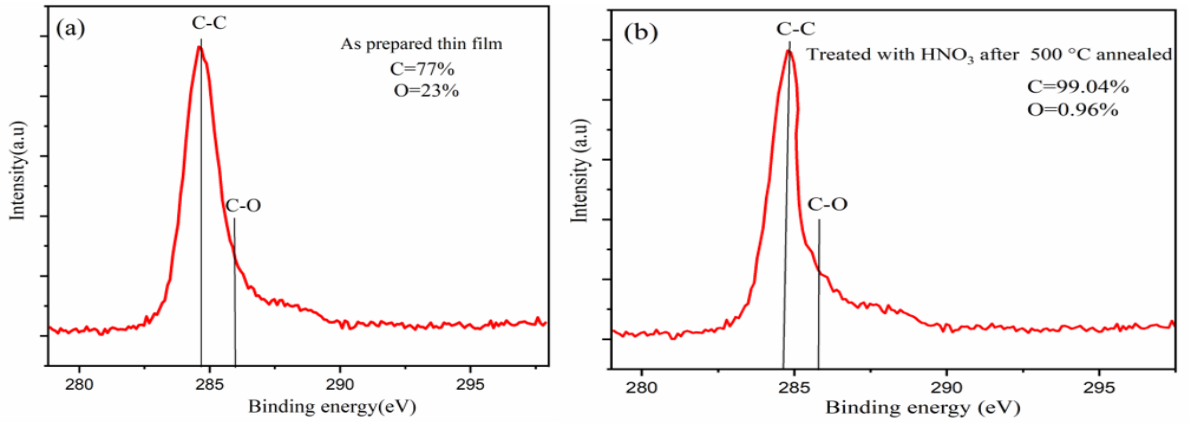

Figure 9: a C1 XPS spectra of as prepared graphene thin film b) C1 XPS spectra of graphene thin film treated with HNO3 after 500°C annealed.

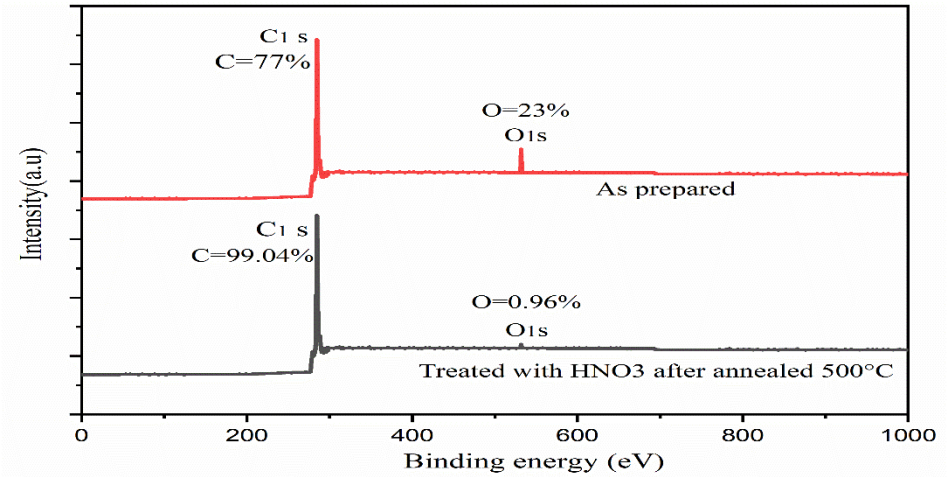

Figure 10: The full-scale XPS spectra of as prepared graphene thin film and graphene thin film treated with HNO_3 after 500°C annealed.

However, the graphene thin films that have been annealed still show a high sheet resistance, making them unsuitable for many technologies. To further reduce graphene thin film resistance, they were treated with HNO_3 to increase the carbon structure's carrier concentration and conductivity; as a result, the graphene thin films treated with HNO3 have less O because of the vigorous oxidation by HNO_3 (Kasry et al., 2010)(Zheng et al., 2011). The sheet resistance of the graphene thin film treated with HNO_3 is 12.2 kΩ/sq, 1.41 kΩ/sq, 1.18 kΩ/sq, and 0.8 kΩ/sq, respectively, as illustrated in Table (1). The XPS spectra of annealed and treated HNO_3 graphene thin film are shown in Figure (9b). The C1 peak of C−C bond emerges at 284.8 eV, and a weak peak C−O bond emerges at 285.9 eV. In general, the as prepared sample examined in XPS shows a broad peak, but the annealed and treated by HNO_3 acid gives shape and a narrow peak relative to the peak of the as prepared one. The sharp peak means that the annealed and treated HNO_3 graphene thin film has a high-intensity C-C bond and a less-intensity C-O bond (Su et al., 2011).

Figure (10) shows that the oxygen peak of annealed and treated HNO_3 graphene thin film is tiny compared to the peak of the as prepared film. In addition, the oxygen content of annealed and HNO_3-treated graphene thin film is only 0.96%, which is lower than that of the as prepared graphene thin film measured by the original software(Li et al., 2016)(Zheng et al., 2014).

4-CONCLUSIONS

This research has indicated that an industrially friendly and environmentally scalable manufacturing of transparent conductor graphene thin films can be grown by an adjusted vacuum filtration process. With a newly improved IDT technique, graphene nanosheets can be transformed easily onto specific substrates such as (glass, and PET). The graphene thin films obtained at the wafer scale exhibited significant quality features, like low sheet resistance, uniform electric conductivity, high excellent transparency, and homogeneity of structure. Various graphene solutions have been used during the process to control the thickness of graphene thin films. SEM images showed that graphene nanosheets are overlapped and stacked to form a conductive platform that allows charge carriers to move. They also illustrated that the graphene nanosheets homogenously deposited without cracks over the entire surface of the graphene nanosheets. The XRD pattern of graphene thin film revealed a diffraction peak at 26.3° and (002) plane, expressing a hexagonal crystal structure of graphene thin film. The graphene thin film's inter-planar distance was slightly bigger (3.39 Å) than that of standard graphite powder (3.35 Å), indicating that re-aggregation had been successfully avoided during thin film fabrication. The sharp diffraction peaks and high intensity confirmed the graphene thin film's crystalline nature and high quality.

A graphene thin film on a glass substrate has a variable transmittance depending on the film thickness. A thicker film with a larger volume of graphene dispersions has a lower transmittance since it absorbs, reflects, and scatters light more intensely. It was found that graphene thin films had transmittances of 81%, 70.6%, 64.3%, and 46.4% at 550nm, with 81% being the maximum. The resistance of as prepared graphene thin films measured by Keithley 2450 four probes were high, about 1000 kΩ/sq, 200 kΩ/sq, 90.5 kΩ/sq, and 21.12 kΩ/sq due to residual solvent and amount of 23% oxygen as XPS analyzes showed. After drying at 500C and treatment with HNO_3, the sheet resistance values decreased significantly. According to XPS analysis, the oxygen content of the HNO_3-treated graphene thin film is only 0.96%, which is lower than that of the as prepared graphene thin film measured by the original software. The minimum electrical sheet resistance is 0.8 kΩ/sq. The treated and annealed films had sheet resistance values of 12.2 kΩ/sq 1.41 kΩ/sq, 1.18 kΩ/sq, and 0.8 kΩ/sq.

REFERENCES

Bae, S., Kim, H., Lee, Y., Xu, X., Park, J.-S., Zheng, Y., Balakrishnan, J., Lei, T., Ri Kim, H., & Song, Y. Il. (2010). Roll-to-roll production of 30-inch graphene films for transparent electrodes. *Nature Nanotechnology*, *5*(8), 574–578.

Baptista-Pires, L., Mayorga-Martínez, C. C., Medina-Sánchez, M., Montón, H., & Merkoçi, A. (2016). Water activated graphene oxide transfer using wax printed membranes for fast patterning of a touch sensitive device. *ACS Nano*, *10*(1), 853–860.

Cai, C., Jia, F., Li, A., Huang, F., Xu, Z., Qiu, L., Chen, Y., Fei, G., & Wang, M. (2016). Crackless transfer of large-area graphene films for superior-performance transparent electrodes. *Carbon*, *98*, 457–462.

Chen, M.-L., Park, C.-Y., Choi, J.-G., & Oh, W.-C. (2011). Synthesis and characterization of metal (Pt, Pd and Fe)-graphene composites. *Journal of the Korean Ceramic*

Society, *48*(2), 147–151.

De, S., Higgins, T. M., Lyons, P. E., Doherty, E. M., Nirmalraj, P. N., Blau, W. J., Boland, J. J., & Coleman, J. N. (2009). Silver nanowire networks as flexible, transparent, conducting films: extremely high DC to optical conductivity ratios. *ACS Nano*, *3*(7), 1767–1774.

Eda, G., Fanchini, G., & Chhowalla, M. (2008a). Large-area ultrathin films of reduced graphene oxide as a transparent and flexible electronic material. *Nature Nanotechnology*, *3*(5), 270–274.

Eda, G., Fanchini, G., & Chhowalla, M. (2008b). Metal-semiconductor contact in organic thin film transistors. *Nat. Nanotechnol.*, *83*, 270–274.

Eda, G., Lin, Y.-Y., Miller, S., Chen, C.-W., Su, W.-F., & Chhowalla, M. (2008). Transparent and conducting electrodes for organic electronics from reduced graphene oxide. *Applied Physics Letters*, *92*(23).

Gutiérrez-Cruz, A., Ruiz-Hernández, A. R., Vega-Clemente, J. F., Luna-Gazcón, D. G., & Campos-Delgado, J. (2022). A review of top-down and bottom-up synthesis methods for the production of graphene, graphene oxide and reduced graphene oxide. *Journal of Materials Science*, *57*(31), 14543–14578.

Han, S., Zhou, Y., Wang, C., He, L., Zhang, W., & Roy, V. A. L. (2013). Layer-by-layer-assembled reduced graphene oxide/gold nanoparticle hybrid double-floating-gate structure for low-voltage flexible flash memory. *Advanced Materials*, *25*(6), 872–877.

Hwangbo, Y., Lee, C.-K., Kim, S.-M., Kim, J.-H., Kim, K.-S., Jang, B., Lee, H.-J., Lee, S.-K., Kim, S.-S., & Ahn, J.-H. (2014). Fracture characteristics of monolayer CVD-graphene. *Scientific Reports*, *4*(1), 4439.

Ito, J., Nakamura, J., & Natori, A. (2008). Semiconducting nature of the oxygen-adsorbed graphene sheet. *Journal of Applied Physics*, *103*(11).

Jo, G., Choe, M., Lee, S., Park, W., Kahng, Y. H., & Lee, T. (2012). The application of graphene as electrodes in electrical and optical devices. *Nanotechnology*, *23*(11), 112001.

Kadhim, K. R., & Mohammed, R. Y. (2022). Effect of Annealing Time on Structure, Morphology, and Optical Properties of Nanostructured CdO Thin Films Prepared by CBD Technique. *Crystals*, *12*(9), 1315.

Kasry, A., Kuroda, M. A., Martyna, G. J., Tulevski, G. S., & Bol, A. A. (2010). Chemical doping of large-area stacked graphene films for use as transparent, conducting electrodes. *ACS Nano*, *4*(7), 3839–3844.

Kholmanov, I. N., Magnuson, C. W., Aliev, A. E., Li, H., Zhang, B., Suk, J. W., Zhang, L. L., Peng, E., Mousavi, S. H., & Khanikaev, A. B. (2012). Improved electrical conductivity of graphene films integrated with metal nanowires. *Nano Letters*, *12*(11), 5679–5683.

Kim, J. Y., Lee, K., Coates, N. E., Moses, D., Nguyen, T.-Q., Dante, M., & Heeger, A. J. (2007). Efficient tandem polymer solar cells fabricated by all-solution processing. *Science*, *317*(5835), 222–225.

Kumar, A., & Zhou, C. (2010). The race to replace tin-doped indium oxide: which material will win? *ACS Nano*, *4*(1), 11–14.

Lee, C., Wei, X., Kysar, J. W., & Hone, J. (2008). Measurement of the elastic properties and intrinsic strength of monolayer graphene. *Science*, *321*(5887), 385–388.

Li, C., Xu, Y.-T., Zhao, B., Jiang, L., Chen, S.-G., Xu, J.-B., Fu, X.-Z., Sun, R., & Wong, C.-P. (2016). Flexible graphene electrothermal films made from electrochemically exfoliated graphite. *Journal of Materials Science*, *51*, 1043–1051.

Liang, J., Huang, Y., Zhang, L., Wang, Y., Ma, Y., Guo, T., & Chen, Y. (2009). Molecular-level dispersion of graphene into poly (vinyl alcohol) and effective reinforcement of their nanocomposites. *Advanced Functional Materials*, *19*(14), 2297–2302.

Liang, X., Sperling, B. A., Calizo, I., Cheng, G., Hacker, C. A., Zhang, Q., Obeng, Y., Yan, K., Peng, H., & Li, Q. (2011). Toward clean and crackless transfer of graphene. *ACS Nano*, *5*(11), 9144–9153.

Nair, R. R., Blake, P., Grigorenko, A. N., Novoselov, K. S., Booth, T. J., Stauber, T., Peres, N. M. R., & Geim, A. K. (2008). Fine structure constant defines visual transparency of graphene. *Science*, *320*(5881), 1308.

Olabi, A. G., Abdelkareem, M. A., Wilberforce, T., & Sayed, E. T. (2021). Application of graphene in energy storage device–A review. *Renewable and Sustainable Energy Reviews*, *135*, 110026.

Parvez, K., Li, R., Puniredd, S. R., Hernandez, Y., Hinkel, F., Wang, S., Feng, X., & Mullen, K. (2013). Electrochemically exfoliated graphene as solution-processable, highly conductive electrodes for organic electronics. *ACS Nano*, *7*(4), 3598–3606.

Pumera, M. (2010). Graphene-based nanomaterials and their electrochemistry. *Chemical Society Reviews*, *39*(11), 4146–4157.

Rafiee, M. A., Rafiee, J., Srivastava, I., Wang, Z., Song, H., Yu, Z., & Koratkar, N. (2010). Fracture and fatigue in graphene nanocomposites. *Small*, *6*(2), 179–183.

Shi, H., Wang, C., Sun, Z., Zhou, Y., Jin, K., & Yang, G. (2015). Transparent conductive reduced graphene oxide thin films produced by spray coating. *Sci. China-Phys. Mech. Astron*, *58*, 14202–14206.

Siburian, R., Simanjuntak, C., Supeno, M., Lumbanraja, S., & Sihotang, H. (2018). *New route to synthesize of graphene nano sheets*.

Simon, P., & Gogotsi, Y. (2008). Materials for electrochemical capacitors. *Nature Materials*, *7*(11), 845–854.

Southard, A., Sangwan, V., Cheng, J., Williams, E. D., & Fuhrer, M. S. (2009). Solution-processed single walled carbon nanotube electrodes for organic thin-film transistors. *Organic Electronics*, *10*(8), 1556–1561. https://doi.org/10.1016/j.orgel.2009.09.001

Su, C.-Y., Lu, A.-Y., Xu, Y., Chen, F.-R., Khlobystov, A. N., & Li, L.-J. (2011). High-quality thin graphene films from fast electrochemical exfoliation. *ACS Nano*, *5*(3), 2332–2339.

Vasanthi, V., Logu, T., Ramakrishnan, V., Anitha, K., & Sethuraman, K. (2020). Study of electrical conductivity and photoelectric response of liquid phase exfoliated graphene thin film prepared via spray pyrolysis route. *Carbon Letters*, *30*, 417–423.

Wang, X., Xiong, Z., Liu, Z., & Zhang, T. (2015). Exfoliation at the liquid/air interface to assemble reduced graphene oxide ultrathin films for a flexible noncontact sensing device. *Advanced Materials*, *27*(8), 1370–1375.

Wang, X., Zhi, L., Tsao, N., Tomović, Ž., Li, J., & Müllen, K. (2008). Transparent carbon films as electrodes in organic solar cells. *Angewandte Chemie International Edition*, *47*(16), 2990–2992.

Xia, J., Chen, F., Li, J., & Tao, N. (2009). Measurement of the quantum capacitance of graphene. *Nature Nanotechnology*, *4*(8), 505–509.

Xia, Z., Leonardi, F., Gobbi, M., Liu, Y., Bellani, V., Liscio, A., Kovtun, A., Li, R., Feng, X., & Orgiu, E. (2016). Electrochemical functionalization of graphene at the nanoscale with self-assembling diazonium salts. *ACS Nano*, *10*(7), 7125–7134.

Xia, Z. Y., Giambastiani, G., Christodoulou, C., Nardi, M. V, Koch, N., Treossi, E., Bellani, V., Pezzini, S., Corticelli,

F., & Morandi, V. (2014). Synergic exfoliation of graphene with organic molecules and inorganic ions for the electrochemical production of flexible electrodes. *ChemPlusChem*, *79*(3), 439–446.

Xueshen, W., Jinjin, L., Qing, Z., Yuan, Z., & Mengke, Z. (2013). Thermal annealing of exfoliated graphene. *Journal of Nanomaterials*, *2013*. https://doi.org/10.1155/2013/101765

Yang, S., Lohe, M. R., Müllen, K., & Feng, X. (2016). New-generation graphene from electrochemical approaches: production and applications. *Advanced Materials*, *28*(29), 6213–6221.

Zhang, P., Ma, L., Fan, F., Zeng, Z., Peng, C., Loya, P. E., Liu, Z., Gong, Y., Zhang, J., & Zhang, X. (2014). Fracture toughness of graphene. *Nature Communications*, *5*(1), 3782.

Zhang, W., Chai, C., Fan, Q., Song, Y., & Yang, Y. (2020). PBCF-Graphene: A 2D Sp2 Hybridized Honeycomb Carbon Allotrope with a Direct Band Gap. *ChemNanoMat*, *6*(1), 139–147.

Zheng, Q. Bin, Gudarzi, M. M., Wang, S. J., Geng, Y., Li, Z., & Kim, J.-K. (2011). Improved electrical and optical characteristics of transparent graphene thin films produced by acid and doping treatments. *Carbon*, *49*(9), 2905–2916.

Zheng, Q., Li, Z., Yang, J., & Kim, J.-K. (2014). Graphene oxide-based transparent conductive films. *Progress in Materials Science*, *64*, 200–247.